Npas4 Is a Novel Activity–Regulated Cytoprotective Factor in Pancreatic β-Cells

Paul V. Sabatini,[1,2] Nicole A.J. Krentz,[1,2] Bader Zarrouki,[3] Clara Y. Westwell-Roper,[1,4] Cuilan Nian,[1,2] Ryan A. Uy,[1] A.M. James Shapiro,[5] Vincent Poitout,[3] and Francis C. Lynn[1,2]

Cellular homeostasis requires intrinsic sensing mechanisms to temper function in the face of prolonged activity. In the pancreatic β-cell, glucose is likely a physiological trigger that activates an adaptive response to stimulation, thereby maintaining cellular homeostasis. Immediate early genes (IEGs) are activated as a first line of defense in cellular homeostasis and are largely responsible for transmitting an environmental cue to a cellular response. Here we examine the regulation and function of the novel β-cell IEG, neuronal PAS domain protein 4 (Npas4). Using MIN6 cells, mouse and human islets, as well as in vivo infusions, we demonstrate that Npas4 is expressed within pancreatic islets and is upregulated by β-cell depolarizing agents. Npas4 tempers β-cell function through a direct inhibitory interaction with the insulin promoter and by blocking the potentiating effects of GLP-1 without significantly reducing glucose-stimulated secretion. Finally, Npas4 expression is induced by classical endoplasmic reticulum (ER) stressors and can prevent thapsigargin- and palmitate-induced dysfunction and cell death. These results suggest that Npas4 is a key activity-dependent regulator that improves β-cell efficiency in the face of stress. We posit that Npas4 could be a novel therapeutic target in type 2 diabetes that could both reduce ER stress and cell death and maintain basal cell function. ***Diabetes*** **62:2808–2820, 2013**

The β-cell is exquisitely sensitive to fluctuations in ambient glucose. Not only does glucose have an essential role in regulating insulin exocytosis, but short-term exposure to glucose has a number of positive effects on β-cells, such as the promotion of insulin expression (1,2), β-cell proliferation (3,4), and survival (5,6). Prolonged exposure to elevated glucose, however, has well-documented detrimental effects on β-cells and causes cellular stress through a number of interrelated pathways, including an increase in endoplasmic reticulum (ER) stress, driven by the unfolded protein response (UPR) (7), a reduction in key genes of glucose sensing such as *Glut2* and glucokinase, a reduction in essential β-cell transcription factors such as Pdx1 (8), increased production of amyloidogenic islet amyloid polypeptide (IAPP) (2,9), and production and secretion of proinflammatory cytokines (10). Prolonged β-cell stress has also recently been demonstrated to lead to a loss of β-cell identity through both transdifferentiation to alternate endocrine cell types and reversion to an endocrine progenitor (11). These findings suggest an important role for homeostatic factors that act to couple β-cell activity to the cellular stress response.

The immediate early genes (IEGs) are the first line of defense against many cellular stresses and activate mechanisms that act to counter the perceived stress (12). By definition, IEGs are regulated by a specific stimulus, such as membrane depolarization, without the requirement for de novo protein synthesis (13). As many of the IEGs are transcription factors, they regulate a second wave of transcription and are critical for translating external signals to functional changes within the cell (14). Although large-scale screens have been used to identify glucose-responsive IEGs in β-cells (15,16), and there has been research on IEG regulation of insulin expression under physiological conditions (17–19), very little research has been conducted on the function of IEGs in maintaining β-cell function in the face of stress (20).

Here we describe the role for the IEG neuronal Per-ARNT-Sim (PAS) domain protein 4 (Npas4) in β-cells. Npas4 is a basic helix-loop-helix transcription factor that is a member of the PAS domain family of factors, which includes Arnt, Clock, BmalI, PASK, Per1, and Hif1a. All of these factors rely on their PAS domain to facilitate signaling in response to the environment and all have been demonstrated to be important for β-cell function (21–25). Although research in neurons has demonstrated that Npas4 is activity regulated (26), critical for contextual fear memory formation (27), and may have cytoprotective functions (28), this report is the first to uncover a role of Npas4 in nonneuronal tissue. We demonstrate that Npas4 is highly induced by activity and stress in β-cells, and we show that Npas4 reduces insulin content, blunts the responsiveness to glucagon-like peptide 1 (GLP-1) and protects β-cells from ER stress. Based on these findings, we believe that Npas4 is an important early mediator of the cellular stress response in β-cells and may offer a new therapeutic target in the treatment of diabetes.

RESEARCH DESIGN AND METHODS

Chemicals. Chemicals were purchased from Fisher Scientific or Sigma-Aldrich. Cell culture reagents and disposables were obtained from Hyclone, LifeTech, BD-Falcon, and Corning.

Animal care and procedures. All procedures were approved by either the University of British Columbia (UBC) or l'Université de Montréal animal care committees. For timed matings, noon on the day the vaginal plug was discovered was considered e0.5. All glucose and intralipid infusions were performed as described by Fontés et al. (29). Islets were isolated from mice at 8–15 weeks of age through standard collagenase digestion.

From the [1]Diabetes Research Group, Child and Family Research Institute, Vancouver, British Columbia, Canada; the [2]Department of Surgery and Department of Cellular and Physiological Sciences, University of British Columbia, Vancouver, British Columbia, Canada; the [3]Montreal Diabetes Research Center, CRCHUM, and Department of Medicine, Université de Montréal, Montréal, Quebec, Canada; the [4]Department of Pathology and Laboratory Medicine, University of British Columbia, Vancouver, British Columbia, Canada; and the [5]Department of Surgery, University of Alberta, Edmonton, Alberta, Canada.

Corresponding author: Francis C. Lynn, francis.lynn@ubc.ca.

Received 5 November 2012 and accepted 28 March 2013.

DOI: 10.2337/db12-1527

This article contains Supplementary Data online at http://diabetes.diabetesjournals.org/lookup/suppl/doi:10.2337/db12-1527/-/DC1.

Immunostaining. Immunostaining was performed on paraformaldehyde (PFA)-fixed, paraffin-embedded tissues as previously described (30). Primary antibodies included rabbit anti-Npas4 (1:350; Abcam), mouse antiglucagon (1:2,000; Sigma-Aldrich), and guinea pig anti-insulin (1:2,000; Millipore). Fluorescently conjugated secondary antibodies were from Jackson ImmunoResearch. Sections were imaged on either a Leica SP5 II confocal imaging system or an Olympus BX61 equipped for widefield fluorescence.

Cell culture. MIN6 cells were cultured in high-glucose Dulbecco's modified Eagle's medium (DMEM) supplemented with 10% FBS, 1× glutamine, and 1× penicillin/streptomycin (pen/strep). Cells were passaged once a week and fed every 2nd day. Islets were cultured in RPMI supplemented with 10% FBS, 1× glutamine, and 1× pen/strep.

Adenovirus construction and infection. Npas4 adenovirus was constructed using the AdEasy system (31). MIN6 cells were infected for 2 h, and cells were then washed with PBS prior to further growth. Islets were picked into experimental plates, and after a 4-h recovery, virus was added and infection took place overnight; media was changed daily. As previously described, all cells were infected with a multiplicity of infection of 100:1 (32).

Real-time PCR. RNA was extracted and purified with TRIzol (LifeTech) according to the manufacturer's protocol. cDNA synthesis was performed using Superscript II (LifeTech). For qPCR, 40 ng of cDNA was amplified using PrimeTime primers/probes (IDT) in a ViiA7 real-time PCR system (ABI); samples were run in triplicate and the expression level was quantified through ΔΔCT determination with *GusB* as a reference gene (33,34). The probe/primer1/primer2 used were as follows: 18s, TGCTCAATCTCGGGTGGCTGAA/GAGACTCTGGCATGCTAACTAG/GGACATCTAAGGGCATCACAG; β-actin, CCCATTCCCACCATCACACCCT/GCCTCGTCACCCACATAG/CTGTATTCCCCTCCATCGTG; Ddit3, CTTGACCCTGCGTCCCTAGCTTG/GCACCTATATGTCATCCCCAG/TGCGTGTGACCTCTGTTG; Gapdh, TGCAAATGGCAGCCCTGGTG/GTGGAGTCATACTGGAACATGTAG/AATGGTGAAGGTCGGTGTG; GusB, TCTAGCTGGAAATGTTCACTGCCCTG/CACCCCTACCACTTACATCG/ACTTTGCCACCCTCATCC; GusB (rat) TGGGCGATCAGCGTCTTGAAGTAAT/GGTCGTGATGTGGTCTGTG/TGTCTGGCGTCATATCTGGTATTG; Ins1, TGTTGGTGCACTTCCTACCCCTG/ATCAGAGACCATCAGCAAGC/GTTTGACAAAAGCCTGGGTG; Ins1 promoter, AGACCTAGCACCAGGCAAGTGTTT/GTGTTGATGTCCAATGAGTGC/CCCATTAAGGTGTCCAGGTG; Ins2, CCTCCACCCAGCTCCAGTTGT/TGATCTACAATGCCACGCTTC/GGCTTCTTCTACACACCCATG; Ins2 promoter, CAGGGAAGTGTTTGGAAACTGCAGC/GGACTAAGTAGAGGTGTTGA/CTGGACTTTGCTGTTTGACC; Ins2 (rat), AAGAATCCACGCTCCCCACACA/CCCAGGCTTTTGTCAAACAG/CACCCAGCTCCAGTTGTG; MafA, ACTTCTCGCTCTCCAGAATGTGCC/AGTCGTGCCGCTTCAAG/CGCCAACTTCTCGTATTTCTCC; NeuroD1, TCATGAGTGCCCAGCTTAATGCCA/TCTTTCGATAGCCATTCGCATC/ATAGTGAAACTGACGTGCCTC; Npas4 (human), ACGCTTCTGCTCAACACTACCGC/GTCCTAATCTACCTGGGCTTTG/CCATCTCTGCCTGAATATCTCC; Npas4, CGTTGGTTCCCCTCCACTTCCAT/GTCTCAACATTCCCCTACGAAG/GACAATATGCCATACTTGAAGACG; Npas4 (rat), CTTGAGCAGAGAGAAGCCCCGTG/ATGAGTCTTGCCTGCATCTAC/ACAAGTAGAAATCCAGGTAGTGC; Pdx1, TTCCGCTGTGTAAGCACCTCCTG/GTACGGGTCCTCTTGTTTTCC/GATGAAATCCACCAAAGCTCAC; Rgs2, AGCGGGAGAAAAGAAGCGGACA/CTGAGAATGCAAAGTGCCATG/AAGTAGCTCAAACGGGTCTTC; Rgs2 enhancer, ATTCGCTCTGGTCAGGCTTGTGT/ATTGTCTTCCCACTGTCACG/GCTGTTTCCTCTATGAGCTGG; Rgs2 intron 1, AGCTCAGAACTAACAATGCAACGTCCA/TGTAGCTGAATAACGTCCACC/TCAACTCAAACATCTCCACCC; Rplp0, TGTCTTCCCTGGGCATCACGTC/TGACATCGTCTTTAAACCCCG/TGTCTGCTCCCACAATGAAG; TBP (human), TCCAAAGGATGCAGAGAAAGCCATCA/GGGAGCATTGGTGAAATAGAATC/GGTTTTGGTCTGGAGTCTGAG.

Western blots. Cells were lysed in standard lysis buffer, and protein was denatured by boiling. Crude lysates were processed using sonication (S-4000 with cuphorn; Misonix) for 2 min (85%) and centrifuged at 10,000*g* for 10 min. Proteins were separated using standard SDS-PAGE and blotted to polyvinylidene fluoride membrane (Bio-Rad). Membranes were blocked with 5% milk powder in Tris-buffered saline with Tween and probed with 1:10,000 rabbit anti-Npas4 (M.E. Greenberg, Harvard University, Cambridge, MA), 1:500 mouse anti-CHOP (Santa Cruz Biotechnology), 1:1,000 chicken anti-Rgs2 (Sigma-Aldrich), 1:2,000 mouse anti-Pdx-1 (Developmental Studies Hybridoma Bank), 1:2,000 mouse anti-NeuroD1 (Cell Signaling), 1:5,000 rabbit anti-MafA (Abcam), or 1:125,000 mouse anti-GAPDH (Sigma-Aldrich) overnight at 4°C. Membranes were then probed with horseradish peroxidase–conjugated secondary antibodies used at a dilution of 1:10,000 (Jackson ImmunoResearch) and visualized using ECL Prime (GE Biosciences). Densiometry was used to quantify protein amounts (ImageJ).

MIN6 cell and islet stimulation. MIN6 cells were seeded at 8.0×10^5 cells/well in 12-well plates (or 2.0×10^5 cells/12-mm coverslip) and cultured for 36 h; media was then changed to low-glucose DMEM. The next morning, cells were stimulated in high-glucose DMEM supplemented with 40 mmol/L KCl. Alternatively, cells were washed with PBS before a 1-h preincubation in HEPES-buffered Krebs-Ringer (KRBH; 114 mmol/L NaCl, 4.7 mmol/L KCl, 1.2 mmol/L KH_2PO_4, 20 mmol/L HEPES, 2.5 mmol/L $CaCl_2$, 0.2% BSA, pH 7.4) supplemented with 2.8 mmol/L glucose. Cells were stimulated with 2.8 or 25 mmol/L glucose-KRBH for 2 h. For cycloheximide (CHX) and EGTA treatment, the preincubation step contained 1.5 μg/mL CHX (60 min) or 5 mmol/L EGTA (10 min). Palmitate was prepared by dissolving palmitic acid in 30 mmol/L NaOH at 70°C, complexing with 20% fatty acid–free BSA (6:1 molar ratio), and dissolution in DMEM. MIN6 cells or mouse islets were cultured overnight and treated with thapsigargin or palmitate as indicated. Groups of 40 overnight-cultured islets were stimulated as described above; 3-h to 24-h stimulations were performed in RPMI. Groups of 50 human islets were handpicked and cultured in Connaught Medical Research Laboratories (5.5 mmol/L glucose) supplemented with pen/strep, glutamine, and 10% FBS. The next morning, islets were treated as above. RNA was extracted or cells were fixed with 4% paraformaldehyde (PFA) for 15 min, permeabilized, and immunostained as described above.

Cell death assay. MIN6 cells were plated onto glass coverslips and infected with virus as above. Forty-eight hours after infection, cells were treated for 24 h with thapsigargin. Cells were fixed, and TUNEL-positive cells were identified using the in situ cell death detection kit (Roche). At least 500 cells from each coverslip were counted to assess TUNEL positivity.

Luciferase assay. MIN6 cells were transfected with 1 μg pFOX-RIPI-Luc (35,36) or pFOX-Luc (promoterless) and 100 ng Npas4-pcDNA3.1 or pcDNA3.1 and 50 ng pCMV-Renilla using Lipofectamine 2000 (LifeTech). After 48 h, cells were lysed with passive lysis buffer (PLB), and luciferase activity was quantified with the Dual Luciferase Reporter assay (Promega) on a SpectraMaxL luminometer (Molecular Devices).

Insulin secretion and cAMP assays. After a 1-h preincubation in KRBH, cells were stimulated for 2 h and KRBH was collected and centrifuged at 2,500*g* for 10 min to remove cellular debris. Supernatants were analyzed with a mouse insulin ELISA (Alpco). Total insulin was determined by acid-ethanol extraction and normalized to total protein content. For cAMP assays, cells were washed once with PBS and stimulated in 0.25 mmol/L isobutylmethylxanthine with or without exendin-4 or forskolin (10 μmol/L) for 30 min in KRBH. Samples were analyzed with a cAMP screen assay kit (LifeTech), and luminescence was detected as above.

Chromatin immunoprecipitation assay. Chromatin immunoprecipitation (ChIP) assays were performed as previously described (37,38). Cells were washed briefly in PBS and then incubated in growth media with or without 40 mmol/L KCl. Cells were then fixed by the addition of 1% formaldehyde in cross-linking buffer (0.1 mol/L NaCl, 1 mmol/L EDTA, 0.5 mmol/L EGTA, 25 mmol/L HEPES-KOH, pH 8.0) for 10 min at room temperature with gentle agitation. Fixation was stopped with the addition of glycine to a final concentration of 125 mmol/L, and incubation continued for 5 min with gentle agitation. Cells were washed three times with ice-cold PBS containing protease inhibitors (Complete EDTA-Free; Roche) and then collected by scraping. Cells were pelleted by centrifugation at 2,000*g* for 10 min at 4°C (PBS decanted), snap frozen in liquid nitrogen, and stored at −80°C. Cells were lysed in 20 cell pellet volumes of L1 buffer (50 mmol/L HEPES-KOH, pH 7.5, 140 mmol/L NaCl, 1 mmol/L EDTA, 10% glycerol, 0.5% NP-40, 0.25% Triton X-100, protease inhibitors) for 10 min at 4°C. The nuclei were pelleted by centrifugation at 3,000*g* for 10 min at 4°C and then rinsed with 20 cell pellet volumes of L2 (200 mmol/L NaCl, 1 mmol/L EDTA, 0.5 mmol/L EGTA, 10 mmol/L Tris-HCl, pH 8.0, protease inhibitors) for 10 min at room temperature and then repelleted as above. Nuclei were resuspended in five cell pellet volumes of L3 (1 mmol/L EDTA, 0.5 mmol/L EGTA, 10 mmol/L Tris-HCl, pH 8.0, protease inhibitors) and sonicated in a Misonix Cup Horn sonicator at 80% power for 24 cycles, 30-s cycles on ice, which resulted in genomic fragments of 200–1 kb in size. Insoluble material was removed by centrifugation at 20,000*g* for 10 min at 4°C. The nuclear lysate was then adjusted to 1 mL by adding L3 buffer supplemented with 0.3 mol/L NaCl, 1% Triton X-100, and 0.1% deoxycholate. The lysate was then precleared by adding 50 μL of prerinsed sheep anti-rabbit Dynabeads (LifeTech) and incubating at 4°C for 1 h with agitation. After preclearing, 5% of the ChIP sample was set aside as input sample, and the remainder of the lysate (950 μL) was incubated with 4 μg of antibody overnight at 4°C. The next day, 40 μL of prerinsed sheep anti-rabbit Dynabeads was added to the immunoprecipitates, and immunoprecipitation was carried out over a second night at 4°C. The bound beads were then washed twice with each of the following: low-salt buffer (150 mmol/L NaCl, 0.1% SDS, 1% Triton X-100, 2 mmol/L EDTA, 20 mmol/L Tris-HCl, pH 8.1), high-salt buffer (500 mmol/L NaCl, 0.1% SDS, 1% Triton X-100, 2 mmol/L EDTA, 20 mmol/L Tris-HCl, pH 8.1), LiCl buffer (0.25 mol/L LiCl, 1% NP-40, 1% deoxycholate, 1 mmol/L EDTA, 10 mmol/L Tris-HCl, pH 8.1), and TE (1 mmol/L EDTA, 10 mmol/L Tris-HCl, pH 8.0). All washes were carried out for 5 min at 4°C. Immunoprecipitated materials were eluted from the beads by adding 200 μL of elution buffer (1% SDS, 0.1 mol/L NaHCO3) and incubating the sample at 65°C with continuous vortexing for 1 h; 150 μL of elution buffer was added to the input

material and processed in parallel. Cross-linking was reversed by overnight incubation at 65°C, and resultant DNA was phenol-chloroform purified, ethanol precipitated, and resuspended in 50 μL TE. One microliter was used for standard Taqman analyses.

Small interfering RNA transfection. Small interfering RNAs (siRNAs; 100 nmol/L) (SMARTpool, ON-TARGETplus no. L-054722; Thermo Scientific) were transfected into MIN6 cells 24 h after plating using HiPerFect (Qiagen) as described in the manufacturer's protocol. Experiments were performed 48 h posttransfection.

Statistical analysis. Prism 5 (GraphPad Software) was used for statistical analysis. Student *t* test and one-way ANOVA with Dunnett test were used, with *P* values ≤0.05 considered significant.

RESULTS

Npas4 is expressed in pancreatic β-cells. Npas4 was initially detected during full-transcriptome analyses of mouse pancreatic islets (39) and is highly expressed compared with other bHLH-PAS domain factors (Fig. 1*A*). Real-time PCR was used to determine when *Npas4* is expressed during β-cell development. As depicted in Fig. 1*B*, *Npas4* is dramatically induced just prior to birth. Immunofluorescence analyses of adult pancreatic sections demonstrated that *Npas4* is expressed in both α- and β-cells but not in the exocrine tissue (Fig. 1*C* and *D* and Supplementary Fig. 1). We noted significant heterogeneity in both the intensity of Npas4 staining between islets and the amount of nuclear staining between islets, suggesting that Npas4 is dynamically regulated.

Npas4 is activity regulated in β-cells. To understand the dynamics of *Npas4* expression in β-cells, MIN6 cells were depolarized with 40 mmol/L potassium chloride (KCl). This glucose-mimicking stimulus caused significant induction, 5- and 50-fold at 20 min and 2 h, respectively, in Npas4 (Fig. 2*A* and *G*). Elevated glucose was unable to significantly increase *Npas4* expression in MIN6 cells after a 12-h preincubation in 5.5 mmol/L glucose (Fig. 2*B* and *G*). Depolarization-induced *Npas4* induction proved calcium dependent as the calcium chelator EGTA prevented induction (Fig. 2*C* and *G*). Induction at the message level was not impacted by blocking protein synthesis, suggesting that Npas4 is an IEG (Fig. 2*D*).

Although glucose did not regulate *Npas4* in MIN6 cells, it dose-dependently increased *Npas4* expression in mouse and human islets with 15- and 40-fold respective increases over basal at 25 mmol/L glucose (Fig. 2*E*, *H*, and *J*). Glucose-induced *Npas4* expression was temporary, returning to baseline levels by 6 h (Fig. 2*F*). Npas4 protein was undetectable under basal conditions, but it was significantly induced by depolarization of both islets and MIN6 cells (compare Fig. 2*G* and *H*). As we noted in both cytoplasmic and nuclear staining from sections of mouse pancreas (Fig. 1*C* and *D*), we depolarized MIN6 with KCl and noted markedly increased nuclear Npas4 immunostaining (Fig. 2*I*).

Npas4 is activity regulated in vivo and induced in a mouse model of diabetes. To confirm these in vitro

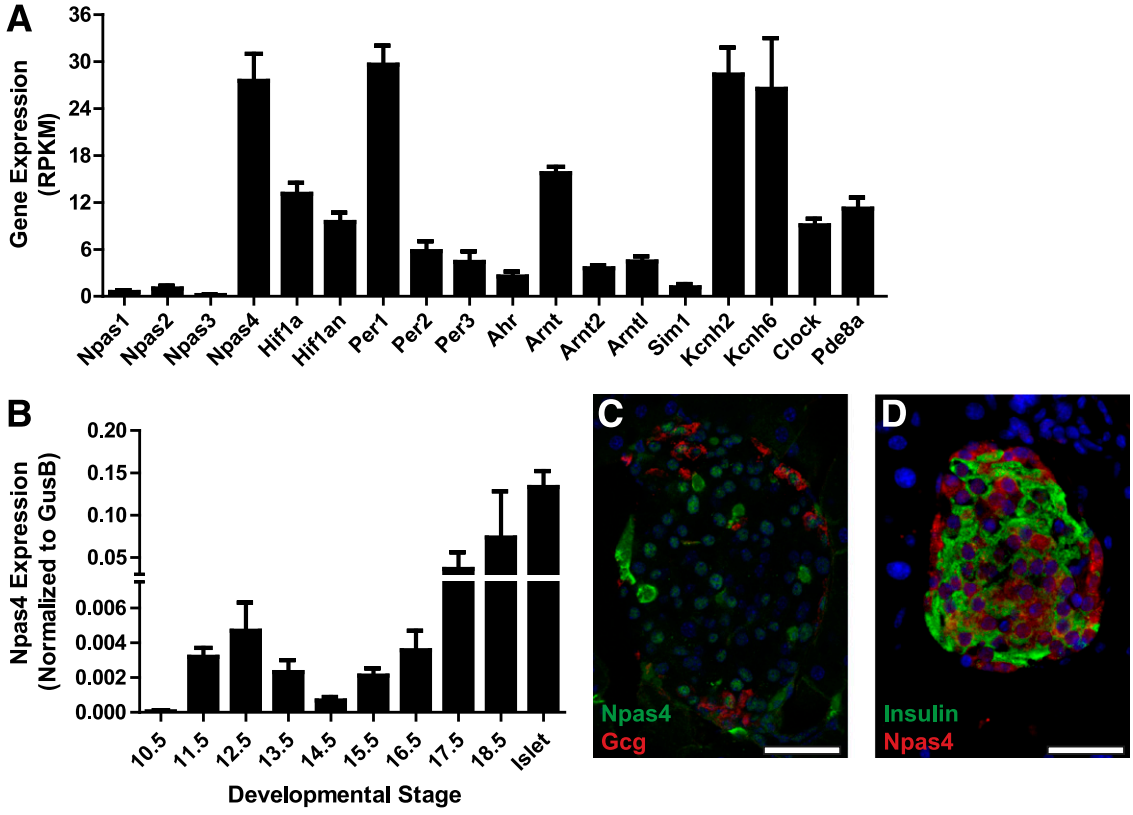

FIG. 1. Npas4 is expressed in β-cells. Compared with other PAS domain factors, *Npas4* was highly expressed in freshly isolated mouse islets ($n = 4$) (*A*). Pancreatic *Npas4* gene expression was induced late in development. Embryonic pancreatic tissue was dissected between e10.5 and e18.5, RNA was extracted and reverse transcribed, and Taqman PCR was carried out for Npas4 ($n = 3–4$) (*B*). Npas4 was restricted to the endocrine pancreas (*C* and *D*). Confocal imaging (*C*) demonstrated that Npas4 (green) colocalized with DNA (blue; DAPI) within glucagon (red)-expressing cells. Widefield immunofluorescence demonstrated that Npas4 (red) colocalized with both DNA (blue) and insulin (green) within pancreatic β-cells (*D*). There was significant variability in the percentage of cells showing Npas4 immunoreactivity within the nucleus in islets within one pancreas, indicating that there is likely nuclear-cytoplasmic shuttling in response to metabolic demands. Scale bars, 50 μm. Gcg, glucagon; RPKM, Reads Per Kilobase of transcript per Million mapped reads.

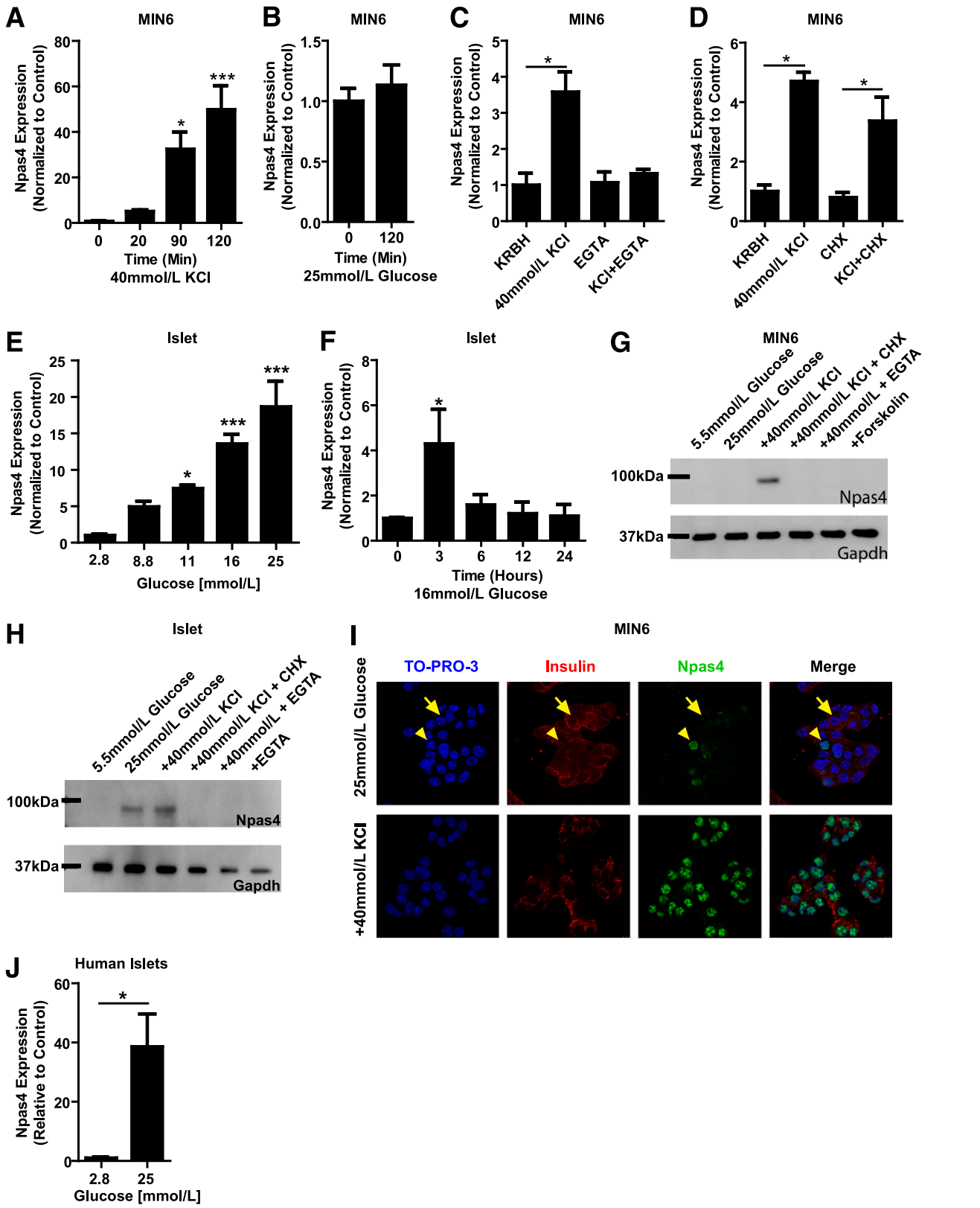

FIG. 2. Npas4 is an activity-regulated transcription factor in pancreatic β-cells. In MIN6 β-cells, a 2-h exposure to 40 mmol/L KCl (n = 4) (*A*) but not 25 mmol/L glucose (n = 3) (*B*) significantly increased *Npas4* gene expression in a calcium-dependent manner (n = 3) (*C*). Further, *Npas4* was induced during the immediate early response in MIN6 cells, as CHX was not able to prevent induction (n = 3) (*D*). In mouse pancreatic islets, *Npas4* was significantly increased by glucose in a dose-dependent fashion (n = 3–8) (*E*) after a 2-h incubation; however, expression levels returned to baseline by 6 h if culture continued in 16 mmol/L glucose (n = 3–4). Npas4 was not appreciably expressed at the protein level in either MIN6 cells (*G*) or mouse islets (*H*) under low glucose (compare *G* and *H*); however, depolarization by KCl in MIN6 cells (n = 3) (*G*) and by both glucose and KCl in mouse islets (n = 3) (*H*) strongly induced expression. In both MIN6 cells and islets (compare *G* and *H*), this induction could be blocked by chelation of calcium with EGTA and by inhibition of protein synthesis (CHX). *I*: Immunofluorescent staining of MIN6 displayed that under basal conditions, Npas4 is mainly cytoplasmic (arrows), with a small percentage of cells containing nuclear Npas4 expression (arrowheads). However,

findings, we used a 72-h in vivo perfusion system. As previously described (29), the jugular vein and carotid artery of 6-month-old Wistar rats were cannulated under general anesthesia and, after a 5-day recovery, infused with saline, 70% glucose, or a 20% lipid emulsion for 72 h. RNA was extracted from freshly isolated islets, cDNA was prepared, and qPCR was performed. *Npas4* expression was significantly elevated in the islets of rats perfused with glucose (Fig. 3*A*), and a trend toward significance was also observed in intralipid-infused animals. Concomitant with the glucose-stimulated induction of *Npas4*, we noted a significant reduction in *Ins2* expression (Fig. 3*B*). To understand if Npas4 is important in diabetes disease progression, we examined Npas4 expression in an obese transgenic mouse model of type 2 diabetes expressing human IAPP under the rat insulin promoter (RIP) in addition to the dominant agouti viable yellow mutation (A^{vy}) (40). Compared with control animals (A^{vy}/A), there was markedly higher expression of Npas4 in the transgenic mice at 14 weeks of age (Fig. 3*C*). By 24 weeks of age, however, there was no appreciable difference observed. In support of these data, Npas4 is upregulated in islets of diabetic mice profiled by the Attie laboratory (http://diabetes.wisc.edu/kelleretal2008/search.php) (41).

Npas4 is a negative regulator of insulin expression. To address whether the in vivo reduction of insulin 2 expression (Fig. 3*B*) could be attributed to an increased expression of *Npas4*, an adenovirus was created to drive Npas4 expression (Ad-Npas4). When compared with KCl-stimulated MIN6 cells infected with a control adenovirus (Ad-Cerulean, variant of GFP), Ad-Npas4 caused an ~40-fold increase in Npas4 protein levels (Supplementary Fig. 2*A*). Ad-Npas4–transduced MIN6 cells showed significantly reduced insulin 1 (38% reduction) and insulin 2 (31% reduction) message levels (Fig. 4*A* and *B*) when normalized to β-glucuronidase expression, an appropriate reference gene for these experiments (Supplementary Fig. 2*B–F*). Insulin content was also reduced by 57% (Fig. 4*C*). Similar results were observed in mouse islets (Fig. 4*D–F*). To determine if endogenous Npas4 tempers insulin expression, we used siRNAs to knock down Npas4 in MIN6 cells; with a 40% reduction in Npas4 protein/mRNA, we observed increases in both *Ins1* and *Ins2* expression (Fig. 4*G* and *H*).

To determine if the negative regulation of insulin by Npas4 was due to decreased transcription, we assessed the ability of Npas4 to regulate expression of RIP1-driven luciferase transcription (35,36). Although there was high luciferase activity in transfected MIN6 cells, cotransfection with Npas4 expression plasmid attenuated luciferase activity to background levels without impacting control, Renilla luciferase activity (Fig. 4*I*). As the decreased promoter activity could be due to either direct or indirect effects, we measured the expression of the three main activators of insulin expression in β-cells: Pdx-1, NeuroD1, and MafA. Although Npas4 overexpression did not alter the mRNA levels of Pdx-1 or NeuroD1 (Fig. 4*J* and *K*), both were significantly reduced at the protein level (Fig. 4*M–P*). Interestingly, there were significant increases in both MafA mRNA and protein levels (Fig. 4*L*, *Q*, and *R*). To test whether Npas4 also had direct effects on insulin promoter activity, we also measured Npas4 enrichment at the insulin promoters with ChIP (38). After a 2-h depolarization with KCl, Npas4 was enriched 11-fold at the insulin 1 (Fig. 4*S* and *T*) promoter and 15-fold at the insulin 2 promoter (Fig. 4*S* and *T*) compared with nondepolarized cells.

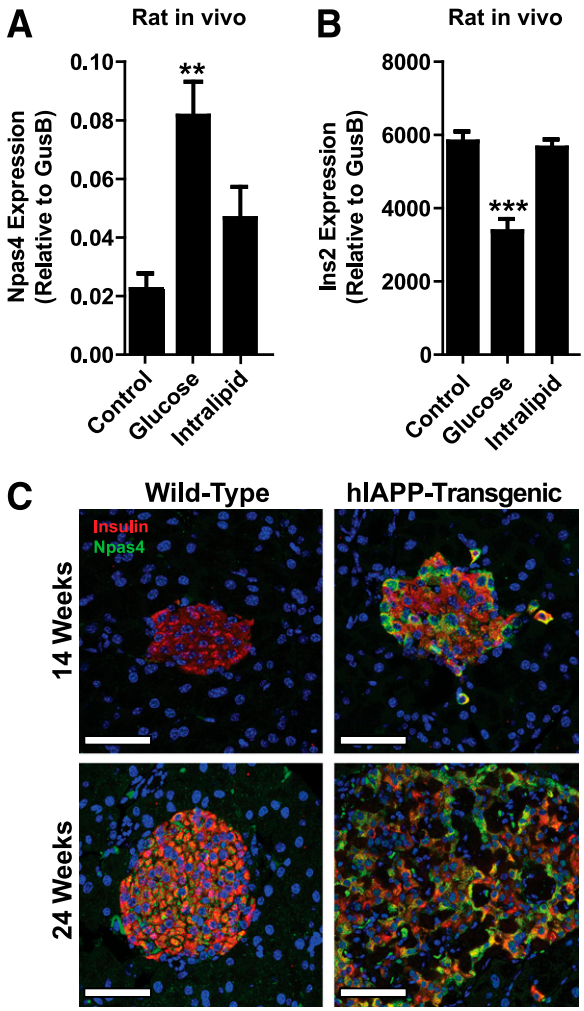

FIG. 3. ***Npas4*** **is induced and Ins2 reduced after 72-h infusion of glucose into live, conscious rats. Under general anesthesia, indwelling catheters were inserted into the left carotid artery and right jugular vein of 6-month-old Wistar rats. The catheters were tunneled subcutaneously and exteriorized at the base of the neck, and the animals recovered for 5 days after surgery. The animals were randomized into three groups, receiving 0.9% saline (control), 70% glucose, or 20% intralipid with heparin (20 units/mL). Initial glucose infusions rates were 3.3 mL · kg^{-1} · h^{-1} and were then adjusted to maintain 13.8–16.7 mmol/L over the 72 h. Lipid infusion rates were 1.7 mL · kg^{-1} · h^{-1}, which were maintained throughout the 72-h infusion. After infusions, islets were isolated, RNA was extracted and reverse transcribed, and Taqman analyses were carried out. Rats infused with glucose had significantly increased *Npas4* expression (*A*) as well as significantly reduced insulin 2 expression (*B*) (n = 4–5). For further evidence of regulation of Npas4 expression in vivo, we examined a model of type 2 diabetes that expresses human IAPP on the heterozygous viable yellow agouti background (hIAPP-A^{vy}/A). Compared with littermate controls (A^{vy}/A mice), at 14 weeks of age, there was significantly higher Npas4 staining in the transgenic group; however, at 24 weeks of age, there was no discernible difference between the two groups (red, insulin; green, Npas4; blue, TO-PRO-3 nuclear dye). Scale bars, 50 μm. Significance was established using a one-way ANOVA with Dunnett post hoc analysis. **$P \le 0.01$; ***$P \le 0.001$.**

under stimulatory conditions, Npas4 is exclusively nuclear, colocalized with TO-PRO-3 nuclear dye (n = 3). Npas4 expression was induced in human islets by 25 mmol/L glucose after a 2-h stimulation (n = 4) (*J*). Significance was established using two-tailed Student t tests or a one-way ANOVA with Dunnett post hoc analysis where applicable. $n \ge 3$. *$P \le 0.05$; ***$P \le 0.001$.

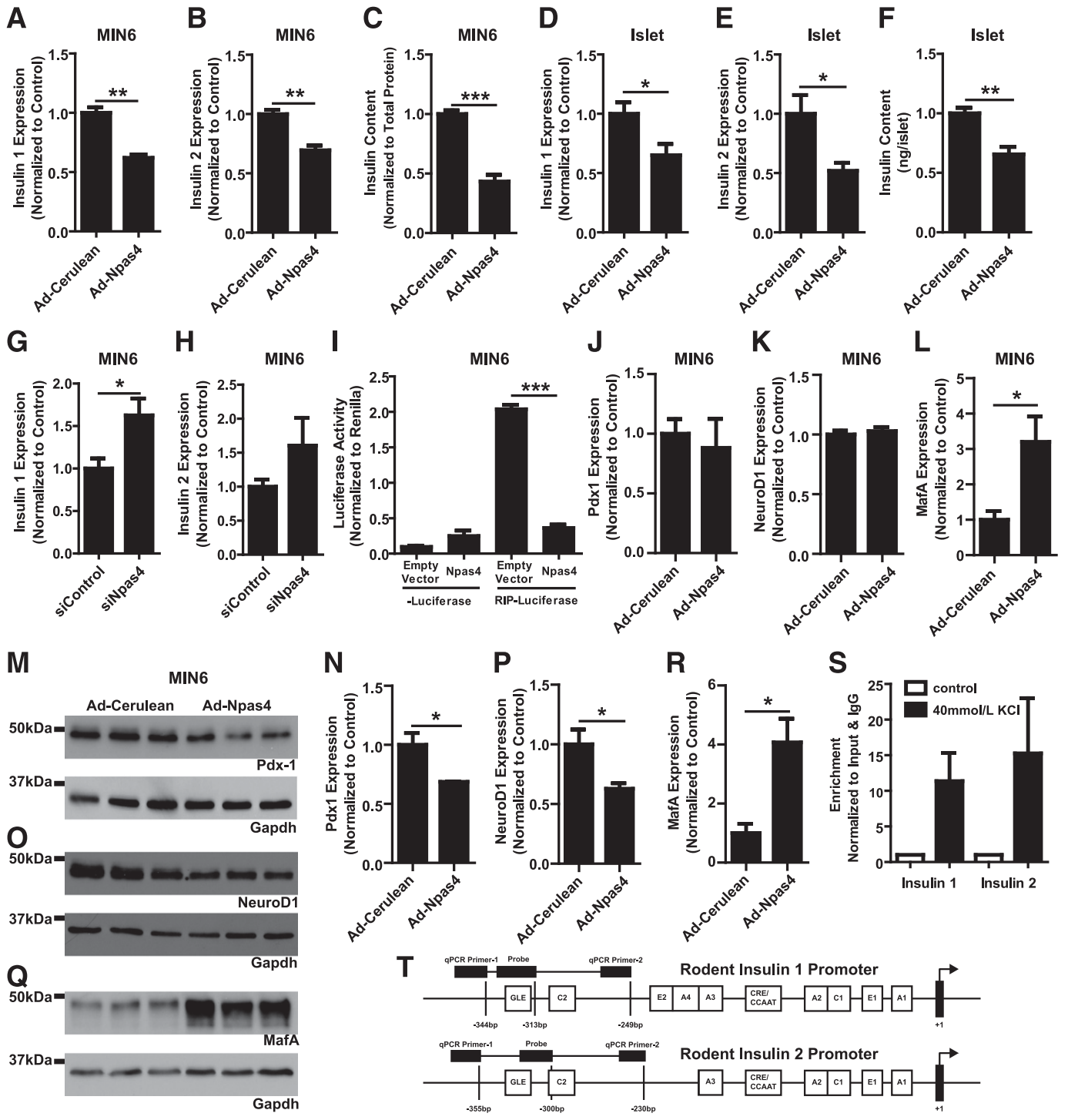

FIG. 4. Npas4 directly regulates insulin gene expression in β-cells. Enforced adenoviral expression of Npas4 in MIN6 cells (*A–C*) significantly decreased expression of insulin 1 (*A*) and insulin 2 (*B*) message levels and total cell content ($n = 3$) (*C*). Adenoviral-driven Npas4 in mouse pancreatic islets (*D–F*) significantly decreased expression of insulin 1 ($n = 4$) (*D*) and insulin 2 ($n = 3$) (*E*) as well as significantly reduced total islet content of insulin ($n = 6$) (*F*). Forty-eight hours after transfection with siRNAs targeting Npas4, increases in both insulin 1 (*G*) and insulin 2 (*H*) expression were observed in MIN6 cells ($n = 4$). Npas4 reduced RIP1-driven luciferase transcription in cotransfected MIN6 cells ($n = 3$) (*I*). Npas4 overexpression in MIN6 did not alter *Pdx-1* (*J*) or *NeuroD1* (*K*) mRNA expression but significantly decreased both at the protein level ($n = 3$) (*M–P*). Npas4 also increased the expression of *MafA* at the message (*L*) and protein (*Q* and *R*) level ($n = 3$). *S*: To determine if Npas4 binds directly to both insulin promoters in MIN6 cells, cells were depolarized for 2 h with 40 mmol/L KCl to induce Npas4, fixed, and chromatin fragmented, and immunoprecipitation was carried out using antibodies specific for Npas4 under both induced (black bars) and control (white bars) conditions. Cross-links were then reverse transcribed, and Taqman PCR was used to assess enrichment at the insulin promoters. Using this approach, there was between 10- and 30-fold enrichment at both promoters ($n = 3$). *T*: Illustrations of quantitative primers and probe binding sites on the insulin 1 and insulin 2 promoter (modified from LeRoith et al. [60]). Significance was determined using two-tailed Student *t* tests. *$P \leq 0.05$; **$P \leq 0.01$; ***$P \leq 0.001$.

Npas4 inhibits incretin-stimulated insulin secretion. Based on the Npas4-induced reduction in insulin content, we hypothesized that there would be defects in insulin secretion. However, when Ad-Npas4–transduced MIN6 cells were stimulated with 16 mmol/L glucose, there was no significant difference in secretion compared with control-infected cells (Fig. 5*A* and *B* and Supplementary Fig. 3). In order to understand if Npas4 could modulate incretin-potentiated secretion, we stimulated cells with the GLP-1 agonist exendin-4. In control conditions, exendin-4 stimulated maximal insulin secretion at 5 nmol/L; however, in Ad-Npas4-transduced MIN6 cells, exendin-4 had no potentiating effects (Fig. 5*A*). Bypassing the GLP-1 receptor and stimulating cAMP production directly with a combination of forskolin and isobutylmethylxanthine (IBMX), which activate adenylyl cyclase and inhibit phosphodiesterase, respectively, was able to partially stimulate secretion in Ad-Npas4–treated cells (Fig. 5*A*). In islets, a significant reduction in exendin-4–potentiated secretion was also observed (Fig. 5*B*). In order to determine if this effect was due to alterations in GLP-1 receptor signaling, we assessed exendin-4–stimulated cAMP production. Ad-Npas4 transduction of MIN6 cells significantly reduced both exendin-4–stimulated (Fig. 5*C*) and forskolin-stimulated (not shown) cAMP production and shifted the EC_{50} value of exendin-4 from 0.76 to 2.65 nmol/L. These data demonstrate that Npas4 regulates the GLP-1 receptor directly but likely plays other roles in modulating cAMP production.

Npas4 increases expression of Rgs2. Based on the ability of Npas4 to inhibit incretin-stimulated cAMP production, we hypothesized that it might induce factors that impair normal receptor–G-protein coupling and examined the GTPase-activating protein Rgs2, which has been previously demonstrated to be a negative regulator of incretin-mediated cAMP production (42). To test if Npas4 regulated *Rgs2*, we measured expression of *Rgs2* after cell depolarization. Under these conditions, *Rgs2* was induced in a time-dependent manner (Fig. 6*A*) with delayed kinetics compared with those for Npas4 (compare Fig. 2*A* and Fig. 6*A*). Regulation of Rgs2 message and protein levels also appeared to be quite similar to Npas4 (compare Fig. 2 and Fig. 6*B* and *C*).

In order to test if *Rgs2* was a target of Npas4, we transduced cells with Ad-Npas4 and observed 16- and 11-fold increases in Rgs2 mRNA in MIN6 cells and mouse islets, respectively (Fig. 6*D* and *E*). We also observed that Ad-Npas4 increased Rgs2 protein expression in MIN6 cells

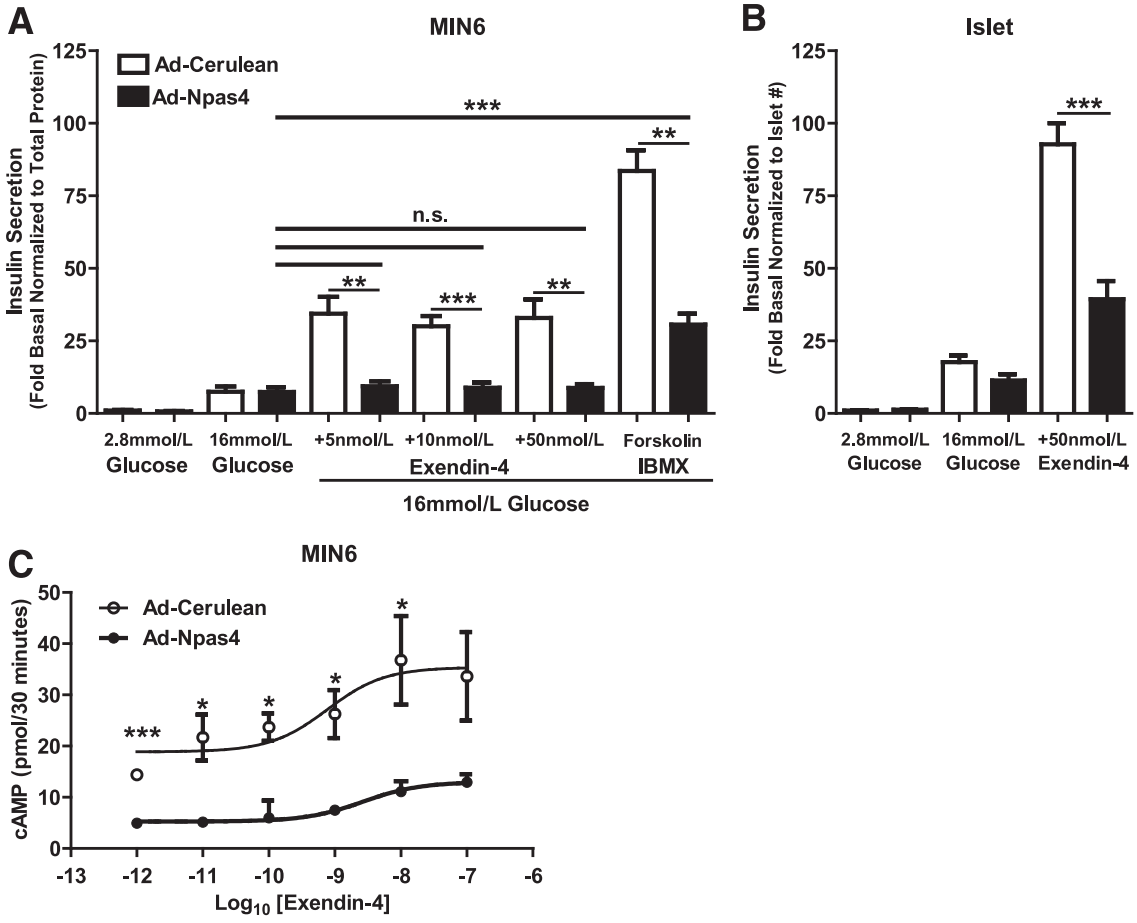

FIG. 5. Npas4 overexpression inhibits β-cell responsiveness to the GLP-1 receptor agonist exendin-4. MIN6 cells were transduced with control (Ad-Cerulean, white bars) or Npas4 (Ad-Npas4, black bars) adenovirus and then cultured for 48 h. No statistical difference was observed in glucose-stimulated insulin secretion in either MIN6 cells (n = 3–5) (*A*) or islets (n = 5–6) (*B*). However, exendin-4–potentiated insulin secretion was reduced after Ad-Npas4 transduction in both MIN6 cells (*A*) and mouse pancreatic islets (*B*). Npas4 overexpression diminished exendin-4–stimulated cAMP production in MIN6, significantly reducing maximal stimulation as well as shifting the EC_{50} from 0.76 to 2.65 nmol/L (n = 3) (*C*). Significance was determined using two-tailed Student t tests or a one-way ANOVA with Dunnett post hoc analysis where applicable. *$P \le 0.05$; **$P \le 0.01$; ***$P \le 0.001$.

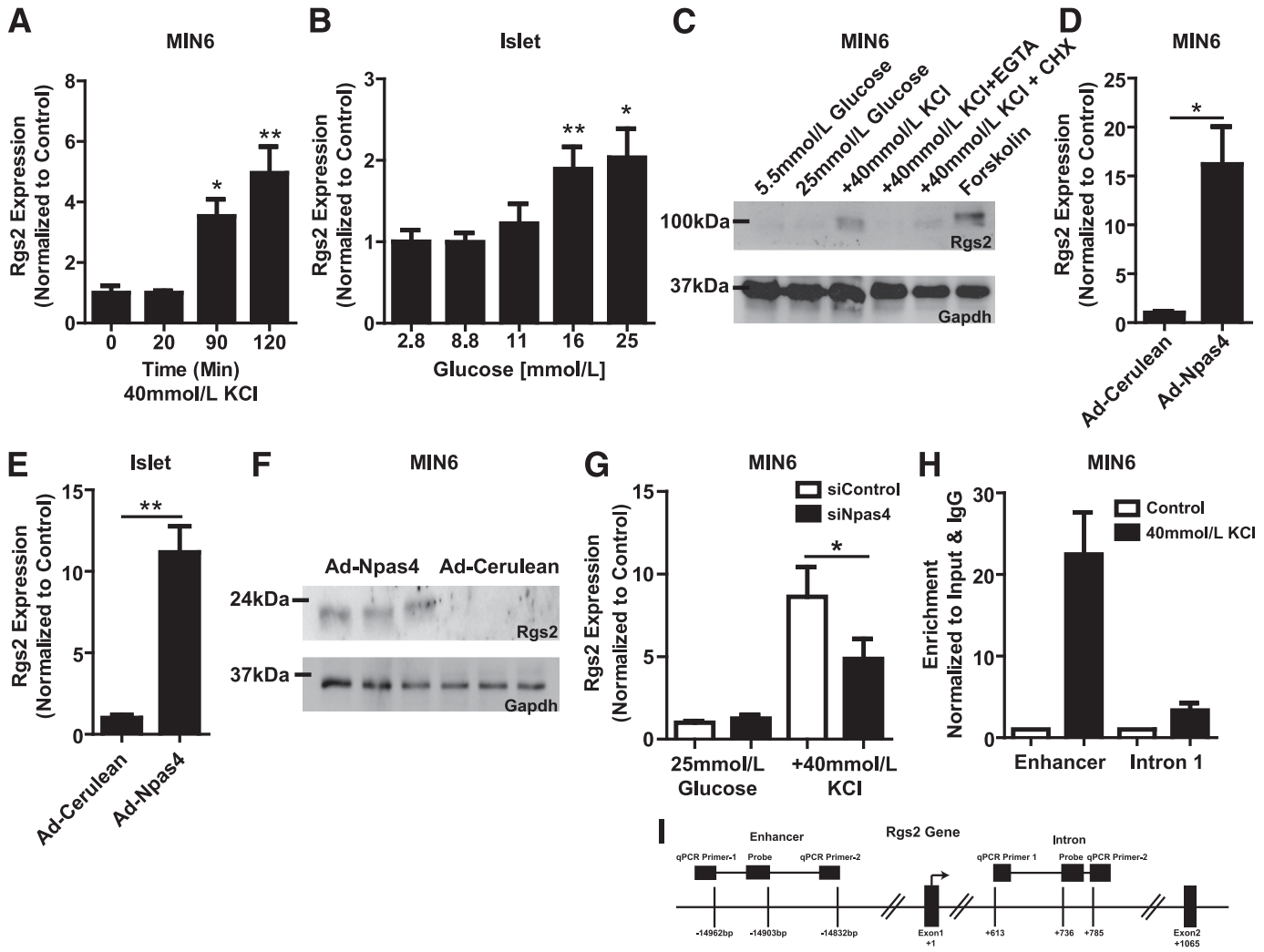

FIG. 6. Npas4 may attenuate incretin-stimulated insulin secretion through the induction of *Rgs2*. *Rgs2* expression was increased in response to 40 mmol/L KCl in MIN6 cells (n = 3) (*A*) and glucose in islets (n = 3–8) (*B*). In MIN6 cells, Rgs2 protein levels were increased in a calcium-dependent manner by KCl as well as forskolin (n = 3) (*C*). Adenovirally overexpressing Npas4 in MIN6 cells (*D*) and islets (*E*) dramatically increased Rgs2 mRNA expression as well as Rgs2 protein levels in MIN6 (n = 3) (*F*). Knockdown of Npas4 in 25 mmol/L glucose did not alter *Rgs2* expression; however, when stimulated with KCl for 2 h, knockdown of Npas4 significantly inhibited the induction of Rgs2 mRNA levels (n = 3) (*G*). Npas4 regulates *Rgs2* through a direct binding to a putative enhancer (15 kb upstream) as well as to the first intron of *Rgs2* as assayed by ChIP (n = 3) (*H*). Illustration of the quantitative primers and probe binding sites in the *Rgs2* gene (*I*). Significance was established using two-tailed Student t tests or a one-way ANOVA with Dunnett post hoc analysis where applicable. *$P \leq 0.05$; **$P \leq 0.01$.

(Fig. 6*F*). Hypothesizing that Npas4 was responsible for the increased *Rgs2* expression under depolarizing conditions, we knocked down Npas4 in MIN6 cells and stimulated with KCl and noted a significantly reduced induction of *Rgs2* (Fig. 6*G*). To assess whether this was a direct effect, we performed ChIP assays after a 2-h depolarization and noted 3- and 22-fold enrichments of Npas4 in intron 1 and in an enhancer (43) of the *Rgs2* gene, respectively (Fig. 6*H* and *I*). Future studies will address how Rgs2 acts to impact GLP-1 receptor function in β-cells.

Npas4 expression is regulated by β-cell stressors. As insulin gene expression comprises ~48% of polyadenylated transcription in the mouse β-cell (unpublished RNA-Seq data), and attenuation of transcription (44) and translation (45) are part of the UPR, we reasoned that the reduction in insulin caused by Npas4 would be advantageous during periods of ER stress.

First, to determine if ER stressors induced Npas4, we treated MIN6 cells with the SERCA pump inhibitor thapsigargin. A 24-h exposure significantly increased *Npas4* expression (Fig. 7*A*). Elevated Npas4 message was observed throughout the 24-h exposure to 1 μmol/L thapsigargin (Fig. 7*B*); however, increased protein expression was only detectable at 24 h (Fig. 7*C*). To test a relevant physiological ER stressor, we exposed MIN6 cells to palmitate (46,47). We observed a dose-dependent increase in *Npas4* expression that peaked at 1 h (15-fold over control with 500 μmol/L palmitate) but was maintained for at least 24 h (Fig. 7*D*). Similar results were noted at the protein level, with palmitate exposure leading to robust induction at 2 h (Fig. 7*E*). Npas4 mRNA levels were also elevated in mouse islets in response to thapsigargin (Fig. 7*F*) and palmitate (Fig. 7*G*).

Npas4 protects β-cells from ER stress. As Npas4 is positively regulated by ER stressors in β-cells, we questioned whether increased *Npas4* expression offered protection from ER stress. As previously demonstrated (46–48), both thapsigargin and palmitate induced the expression of the proapoptotic transcription factor *Ddit3* (i.e., CHOP/GADD153) (Fig. 8*A* and *B*). However, Ad-Npas4 transduction

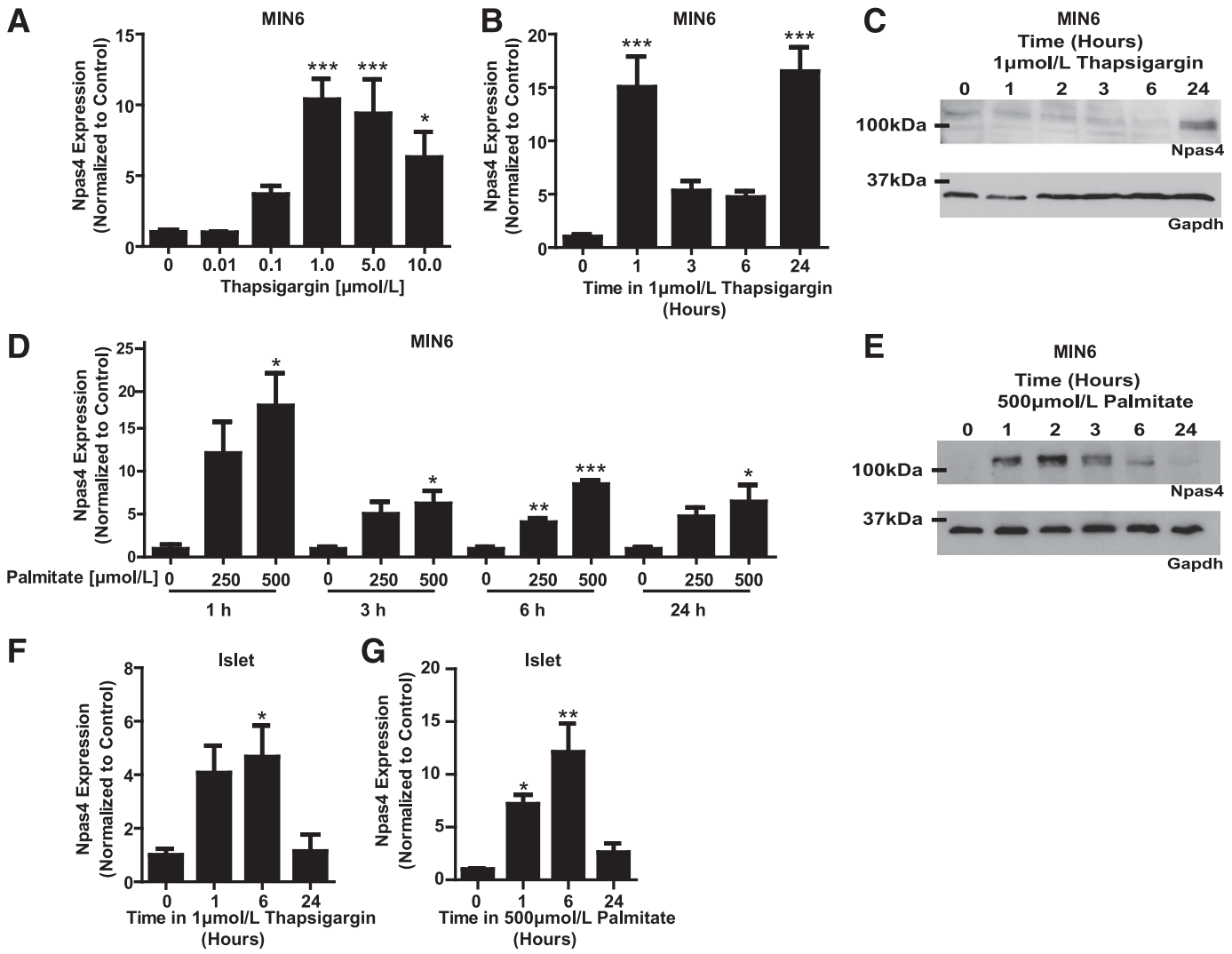

FIG. 7. Npas4 is a stress-induced factor in pancreatic β-cells. *Npas4* expression was induced in a dose-dependent manner in MIN6 cells by a 24-h exposure to the ER calcium–depleting drug thapsigargin (n = 3–6) (*A*). However, in 1 μmol/L thapsigargin, the Npas4 response is dynamic, with markedly higher expression at 1 and 24 h at the message level (*B*) and 24 h at the protein level (n = 3) (*C*). *Npas4* was also induced in a dose-dependent manner by palmitate with maximum expression between 1 and 2 h at both the message (*D*) and protein (n = 3) (*E*) levels in response to 500 μmol/L palmitate. Elevated expression was maintained through 24 h (compare *D* and *E*) (n = 3). In mouse islets, *Npas4* expression was increased after 24-h exposure to 1 μmol/L thapsigargin (*F*) and 500 μmol/L palmitate (n = 3) (*G*) in 11 mmol/L glucose RPMI. Significance was established using two-tailed Student t tests or a one-way ANOVA with Dunnett post hoc analysis where applicable. *$P \leq 0.05$; **$P \leq 0.01$; ***$P \leq 0.001$.

reduced *Ddit3* significantly in MIN6 cells (Fig. 8*A* and *B*). Ad-Npas4 also resulted in a 53% reduction in Ddit3 protein levels in thapsigargin-treated MIN6 cells (Fig. 8*C* and *D*). Knockdown of Npas4 did not change basal *Ddit3* expression; although after palmitate exposure, Ddit3 was significantly increased upon Npas4 knockdown (Fig. 8*E*). Furthermore, Ad-Npas4 reduced thapsigargin- and palmitate-driven expression of *ATF4* and *Xbp-1* (Supplementary Fig. 4) and increased expression of the cytoprotective factors *Wfs-1* and *Hspa5* (Fig. 8*F* and *G*). In isolated mouse islets, Npas4 transduction reduced *Ddit3* expression induced by both thapsigargin and palmitate (Fig. 8*H* and *I*). As Ddit3 is a proapoptotic transcription factor and a terminal step in the ER stress pathway, we next determined if there were any alterations in β-cell apoptosis. Ad-Npas4 significantly reduced the number of $TUNEL^+$ apoptotic MIN6 cells to 68.4 and 55% of control levels with 1 and 10 μmol/L thapsigargin, respectively (Fig. 8*J*).

DISCUSSION

Although previously considered to be brain specific, we demonstrate that *Npas4* is expressed in β-cells and induced after glucose-mediated depolarization in a calcium-dependent manner. Further, we have demonstrated that Npas4 is a novel factor capable of directly and indirectly inhibiting insulin promoter activity and reducing insulin content without significantly affecting glucose-stimulated secretion. Npas4 appears to reduce β-cell stress and prevent β-cell death by blunting incretin-stimulated cAMP production and potentiation of insulin secretion and by counteracting ER stress.

Under normal physiological conditions, elevation in blood glucose levels would stimulate β-cell insulin production and secretion and subsequent rapid (<2 h) normalization of blood glucose to basal levels. In these circumstances, we expect that Npas4 may be induced to efficiently couple insulin supply and demand and reduce the likelihood that insulin biosynthesis places undue stress

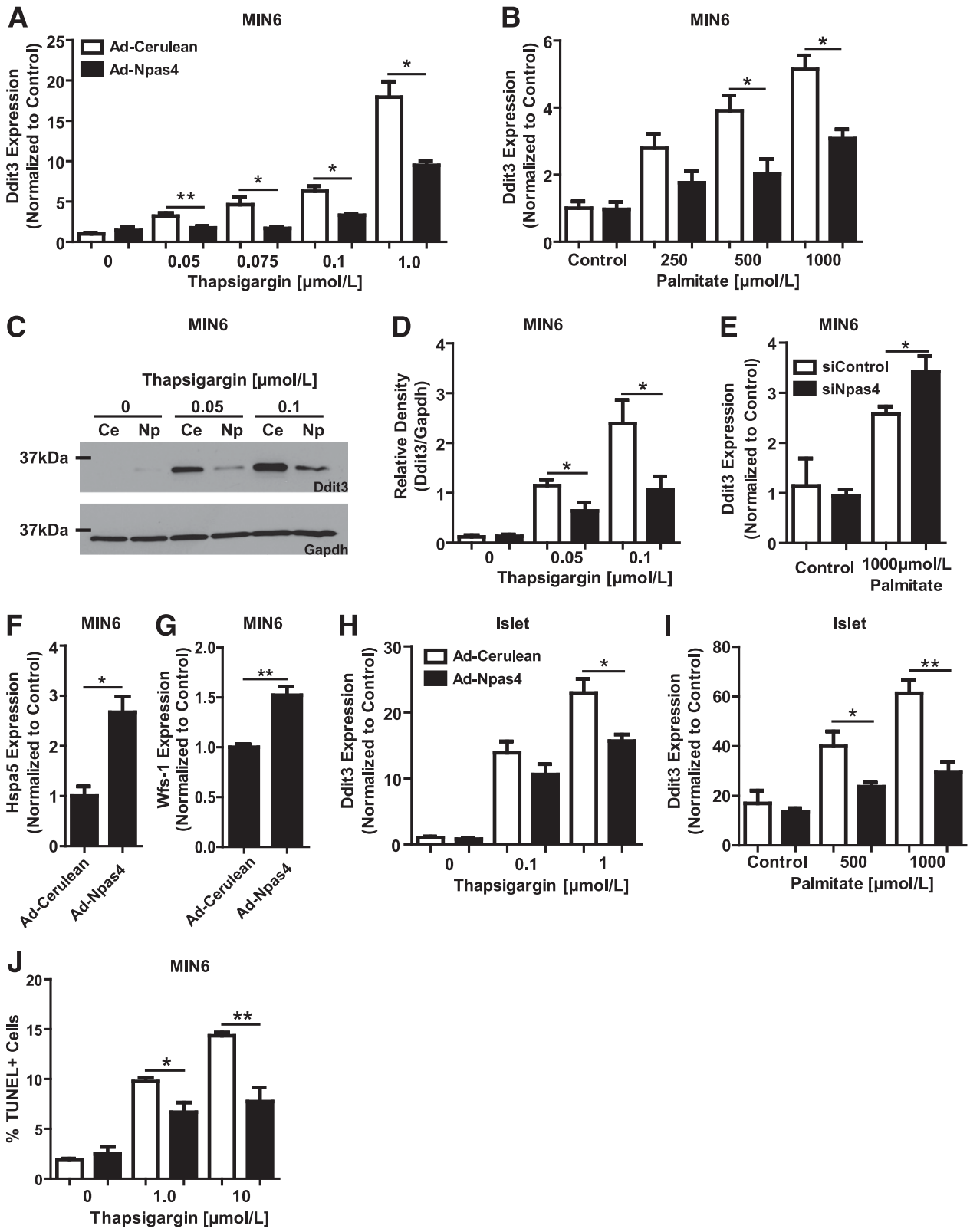

FIG. 8. Npas4 induction is cytoprotective for pancreatic β-cells. Npas4 overexpression (black bars) in MIN6 cells (*A*, *B*, and *D*) significantly reduced *Ddit3* induction after both thapsigargin (n = 3–10) (*A*) and palmitate (n = 3–5) (*B*) exposure. *C* and *D*: The reductions observed at the message level were also present at the protein level as adenoviral transduction with Npas4 (Np) decreased thapsigargin-mediated Ddit3 induction compared with controls (Ce) (n = 3–4). Knockdown of Npas4 with siRNAs did not alter basal Ddit3 expression but, after palmitate exposure, significantly increased Ddit3 levels (n = 4) (*E*). A possible mechanism for the reduced *Ddit3* induction is due to significant increases of the cytoprotective proteins BiP and Wfs-1 (n = 3) (*F* and *G*). Less *Ddit3* induction in response to thapsigargin (n = 6–11) (*H*) or palmitate (n = 3–4) (*I*) was observed in mouse pancreatic islets after Ad-Npas4 transduction. The reductions in Ddit3 mRNA and protein translated to significantly reduced TUNEL$^+$ apoptotic MIN6 cells in Ad-Npas4–infected cells treated with either 1 or 10 μmol/L thapsigargin (n = 3) (*J*). Significance was determined using two-tailed Student t tests. *$P \le 0.05$; **$P \le 0.01$.

on the cells (49). As demonstrated here, a reduction in incretin-potentiated secretion and insulin production could help mediate these effects. Interestingly, we did not observe a significant detriment in glucose-stimulated insulin secretion when we drove Npas4 expression in β-cells, supporting the concept that induction of Npas4 likely improves the "fuel efficiency" of β-cells.

Improvement of β-cell function through reducing insulin demand has long been an attractive approach for treating diabetes. Indeed, work published in 1976 in the Lancet demonstrated that a 7-day administration of the K_{ATP} channel opener diazoxide to people with type 2 diabetes improved the posttreatment insulin secretory response (50). More recently, it has been demonstrated that in people newly diagnosed with type 2 diabetes, a 2-year treatment course of insulin, but not glibenclamide, improved glycemic outcomes (51). In addition, costimulation of murine β-cell lines with diazoxide and palmitate attenuated the following: the palmitate-induced reduction in insulin secretion, the palmitate-induced ER stress, and subsequent apoptosis (52). In order to understand how the immediate early response might help maintain β-cell function, future studies should be targeted at understanding whether loss of Npas4, or other IEGs, increases β-cell susceptibility to stress in vivo.

Prolonged exposure to glucose resulted in a desensitization of the Npas4 response and a return to baseline levels, a characteristic common to activity-regulated IEGs (17,20,26,53). Under normal physiological conditions, the β-cell would not endure high glucose levels for >6 h, and it is likely that Npas4 target genes would be maximally activated under such conditions. It is possible that the gluco (lipo)toxicity/dysfunction that has previously been reported to cause β-cell dysfunction during the development of type 2 diabetes is actually a homeostatic mechanism that acts to protect β-cells. Furthermore, this response may be initiated quite early on with expression of IEGs such as Npas4.

Studies using multiple rodent models of type 2 diabetes suggest that β-cell failure is driven by ER stress–induced dysfunction and death (54). In this manuscript, we demonstrate that Npas4 is induced through exposure to calcium-mobilizing β-cell ER stressors such as thapsigargin and palmitate. We reasoned that because Npas4 can reduce insulin biosynthesis, it might be able to protect against ER stress without significant detrimental physiological effects.

Ddit3 is a transcription factor that is induced by ER stress through prolonged activation of the protein kinase RNA-like endoplasmic reticulum kinase (PERK) arm of the UPR (49). Ddit3 induces apoptosis by driving expression of proapoptotic genes (e.g., *Bim*) and reducing the expression of antiapoptotic genes (55). The induction of *Ddit3* has been demonstrated to be a key step in the development of type 2 diabetes as its genetic deletion protects from diabetes in both the *db/db* mouse and the high-fat diet/streptozotocin-treated mouse (56). Furthermore, a recent study suggested that the GLP-1 agonist liraglutide reduced β-cell ER stress (57); it is currently unclear whether this is a direct or secondary effect of GLP-1 signaling as an immediate effect was not observed. Additionally, it is unclear whether downregulation of β-cell GLP-1 receptor signaling after long-term stimulation might help mediate this effect.

Overexpression of Npas4 reduced the induction of *Ddit3* and *Xbp1* and the splicing of Xbp1 and reduced β-cell death in response to ER stress. Although we did not directly measure *Atf6* expression, it is likely that this arm of the UPR is also affected by Npas4 as we observed significant induction of *Xbp*, the chaperone *Hspa5*, and *Wfs-1*, which may not be primarily induced by the other arms (49). *MafA* was induced by Npas4 and likely contributes to cytoprotection, as MafA directly inhibits *Ddit3* promoter activity in β-cells (58). Interestingly, another novel cytoprotective factor (ARC) was recently described that also acts by potently suppressing Ddit3 expression in β-cells (59). It will be interesting to determine if both *ARC* and *MafA* are direct Npas4 targets.

Current treatment strategies for type 2 diabetes are targeted toward driving β-cell activity in the face of already elevated cellular stress. Although this strategy has produced drugs that increase insulin secretion and β-cell function over the short-term, recent research has suggested that this approach may exacerbate β-cell failure over the long-term. For example, Talchai et al. (11) demonstrated that β-cells in models of diabetes lose their identity after chronic stress and dedifferentiate. In conclusion, we propose that a complimentary therapeutic strategy to those currently used for type 2 diabetes would be to reduce ER stress and β-cell death while maintaining β-cell function. We posit that Npas4 may offer a therapeutic means to accomplish this goal.

ACKNOWLEDGMENTS

This work was supported by grants to F.C.L. from the Juvenile Diabetes Research Foundation (2-2011-91) and the Canadian Institutes of Health Research (CIHR) (MOP 102628) and to V.P. from the U.S. National Institutes of Health (R01-DK-58096). V.P. holds the Canada Research Chair in Diabetes and Pancreatic Beta-Cell Function. The Michael Smith Foundation for Health Research, the Canadian Diabetes Association, and the Child and Family Research Institute (Vancouver, British Columbia) provided salary support for F.C.L. P.V.S. and N.A.J.K. were recipients of the CIHR-BC Transplantation Trainee Fellowship, and R.A.U. was a recipient of the Child and Family Research Institute (Vancouver, British Columbia) undergraduate studentship. C.Y.W.-R. was supported by a CIHR-Vanier Canada Graduate Scholarship.

B.Z. received postdoctoral fellowship support from Merck Frosst and Eli Lilly. No other potential conflicts of interest relevant to this article were reported.

P.V.S. performed experiments and wrote the manuscript. N.A.J.K., B.Z., C.Y.W.-R., C.N., and R.A.U. performed experiments. A.M.J.S. and V.P. provided reagents. F.C.L. designed, directed, and performed experiments and wrote the manuscript. All authors subsequently edited the manuscript. F.C.L. is the guarantor of this work and, as such, had full access to all the data in the study and takes responsibility for the integrity of the data and the accuracy of the data analysis.

The authors thank Dr. Bruce Verchere, University of British Columbia, Vancouver, British Columbia, Canada; Dr. Michael S. German, University of California, San Francisco, San Francisco, California; Dr. Stuart B. Smith, University of California, San Francisco, San Francisco, California; and Dr. Michael E. Greenberg, Harvard University, Cambridge, Massachusetts, for their generous contributions of reagents that made this work possible.

REFERENCES

1. Muller D. Identification of insulin signaling elements in human cells: autocrine regulation of insulin gene expression. Diabetes 2006;55:2835–2842
2. Alarcon C, Verchere CB, Rhodes CJ. Translational control of glucose-induced islet amyloid polypeptide production in pancreatic islets. Endocrinology 2012;153:2082–2087
3. Levitt H, Cyphert T, Pascoe J, et al. Glucose stimulates human beta cell replication in vivo in islets transplanted into NOD–severe combined immunodeficiency (SCID) mice. Diabetologia 2011;54:572–582
4. Porat S, Weinberg-Corem N, Tornovsky-Babaey S, et al. Control of pancreatic β cell regeneration by glucose metabolism. Cell Metab 2011;13:440–449
5. Hoorens A, Van de Casteele M, Klöppel G, Pipeleers D. Glucose promotes survival of rat pancreatic beta cells by activating synthesis of proteins which suppress a constitutive apoptotic program. J Clin Invest 1996;98:1568–1574
6. Srinivasan S, Bernal-Mizrachi E, Ohsugi M, Permutt MA. Glucose promotes pancreatic islet β-cell survival through a PI 3-kinase/Akt-signaling pathway. Am J Physiol Endocrinol Metab 2002;283:E784–E793
7. Tang C, Koulajian K, Schuiki I, et al. Glucose-induced beta cell dysfunction in vivo in rats: link between oxidative stress and endoplasmic reticulum stress. Diabetologia 2012;55:1366–1379
8. Zangen DH, Bonner-Weir S, Lee CH, et al. Reduced insulin, GLUT2, and IDX-1 in β-cells after partial pancreatectomy. Diabetes 1997;46:258–264
9. Janson J, Soeller WC, Roche PC, et al. Spontaneous diabetes mellitus in transgenic mice expressing human islet amyloid polypeptide. Proc Natl Acad Sci USA 1996;93:7283–7288
10. Maedler K, Sergeev P, Ris F, et al. Glucose-induced B cell production of IL-1β contributes to glucotoxicity in human pancreatic islets. J Clin Invest 2002;110:851–860
11. Talchai C, Xuan S, Lin HV, Sussel L, Accili D. Pancreatic β cell dedifferentiation as a mechanism of diabetic β cell failure. Cell 2012;150:1223–1234
12. Fowler T, Sen R, Roy AL. Regulation of primary response genes. Mol Cell 2011;44:348–360
13. Greenberg ME, Hermanowski AL, Ziff EB. Effect of protein synthesis inhibitors on growth factor activation of c-fos, c-myc, and actin gene transcription. Mol Cell Biol 1986;6:1050–1057
14. Morgan JI, Curran T. Stimulus-transcription coupling in neurons: role of cellular immediate-early genes. Trends Neurosci 1989;12:459–462
15. Glauser DA, Brun T, Gauthier BR, Schlegel W. Transcriptional response of pancreatic beta cells to metabolic stimulation: large scale identification of immediate-early and secondary response genes. BMC Mol Biol 2007;8:54
16. Susini S, Roche E, Prentki M, Schlegel W. Glucose and glucoincretin peptides synergize to induce C-Fos, C-Jun, junB, Zif-268, and Nur-77 gene expression in pancreatic β(INS-1) cells. FASEB J 1998;12:1173–1182
17. Müller I, Rössler OG, Wittig C, Menger MD, Thiel G. Critical role of Egr transcription factors in regulating insulin biosynthesis, blood glucose homeostasis, and islet size. Endocrinology 2012;153:3040–3053
18. Eto K, Kaur V, Thomas MK. Regulation of insulin gene transcription by the immediate-early growth response gene Egr-1. Endocrinology 2006;147:2923–2935
19. Sarkar A, Zhang M, Liu SH, et al. Serum response factor expression is enriched in pancreatic β cells and regulates insulin gene expression. FASEB J 2011;25:2592–2603
20. Briand O, Helleboid-Chapman A, Ploton M, et al. The nuclear orphan receptor Nur77 is a lipotoxicity sensor regulating glucose-induced insulin secretion in pancreatic cells. Mol Endocrinol 2012;26:399–413
21. Marcheva B, Ramsey KM, Buhr ED, et al. Disruption of the clock components CLOCK and BMAL1 leads to hypoinsulinaemia and diabetes. Nature 2010;466:627–631
22. Gunton JE, Kulkarni RN, Yim S, et al. Loss of ARNT/HIF1β mediates altered gene expression and pancreatic-islet dysfunction in human type 2 diabetes. Cell 2005;122:337–349
23. Chen H, Houshmand G, Mishra S, Fong GH, Gittes GK, Esni F. Impaired pancreatic development in Hif2-alpha deficient mice. Biochem Biophys Res Commun 2010;399:440–445
24. Cheng K, Ho K, Stokes R, et al. Hypoxia-inducible factor-1 alpha regulates beta cell function in mouse and human islets. J Clin Invest 2010;120:2171–2183
25. Fontés G, Semache M, Hagman DK, et al. Involvement of per-Arnt-Sim kinase and extracellular-regulated kinases-1/2 in palmitate inhibition of insulin gene expression in pancreatic β-cells. Diabetes 2009;58:2048–2058
26. Lin Y, Bloodgood BL, Hauser JL, et al. Activity-dependent regulation of inhibitory synapse development by Npas4. Nature 2008;455:1198–1204
27. Ramamoorthi K, Fropf R, Belfort GM, et al. Npas4 regulates a transcriptional program in CA3 required for contextual memory formation. Science 2011;334:1669–1675
28. Ooe N, Motonaga K, Kobayashi K, Saito K, Kaneko H. Functional characterization of basic helix-loop-helix-PAS type transcription factor NXF in vivo: putative involvement in an "on demand" neuroprotection system. J Biol Chem 2008;284:1057–1063
29. Fontés G, Zarrouki B, Hagman DK, et al. Glucolipotoxicity age-dependently impairs beta cell function in rats despite a marked increase in beta cell mass. Diabetologia 2010;53:2369–2379
30. Lynn FC, Skewes-Cox P, Kosaka Y, McManus MT, Harfe BD, German MS. MicroRNA expression is required for pancreatic islet cell genesis in the mouse. Diabetes 2007;56:2938–2945
31. Luo J, Deng Z-L, Luo X, et al. A protocol for rapid generation of recombinant adenoviruses using the AdEasy system. Nat Protoc 2007;2:1236–1247
32. Gasa R, Mrejen C, Leachman N, et al. Proendocrine genes coordinate the pancreatic islet differentiation program in vitro. Proc Natl Acad Sci USA 2004;101:13245–13250
33. Miyatsuka T, Li Z, German MS. Chronology of islet differentiation revealed by temporal cell labeling. Diabetes 2009;58:1863–1868
34. Ohta Y, Kosaka Y, Kishimoto N, et al. Convergence of the insulin and serotonin programs in the pancreatic cell. Diabetes 2011;60:3208–3216
35. Mauvais-Jarvis F, Smith SB, Le May C, et al. PAX4 gene variations predispose to ketosis-prone diabetes. Hum Mol Genet 2004;13:3151–3159
36. Griffen SC, Wang J, German MS. A genetic defect in β-cell gene expression segregates independently from the fa locus in the ZDF rat. Diabetes 2001;50:63–68
37. Flavell SW, Kim T-K, Gray JM, et al. Genome-wide analysis of MEF2 transcriptional program reveals synaptic target genes and neuronal activity-dependent polyadenylation site selection. Neuron 2008;60:1022–1038
38. Lynn FC, Smith SB, Wilson ME, Yang KY, Nekrep N, German MS. Sox9 coordinates a transcriptional network in pancreatic progenitor cells. Proc Natl Acad Sci USA 2007;104:10500–10505
39. Kim H, Toyofuku Y, Lynn FC, et al. Serotonin regulates pancreatic beta cell mass during pregnancy. Nat Med 2010;16:804–808
40. Soeller WC, Janson J, Hart SE, et al. Islet amyloid-associated diabetes in obese A(vy)/a mice expressing human islet amyloid polypeptide. Diabetes 1998;47:743–750
41. Keller MP, Choi Y, Wang P, et al. A gene expression network model of type 2 diabetes links cell cycle regulation in islets with diabetes susceptibility. Genome Res 2008;18:706–716
42. Tseng C-C, Zhang X-Y. Role of regulator of G protein signaling in desensitization of the glucose-dependent insulinotropic peptide receptor. Endocrinology 1998;139:4470–4475
43. Kim T-K, Hemberg M, Gray JM, et al. Widespread transcription at neuronal activity-regulated enhancers. Nature 2010;465:182–187
44. Hollien J. Decay of endoplasmic reticulum-localized mRNAs during the unfolded protein response. Science 2006;313:104–107
45. Harding HP, Zhang Y, Bertolotti A, Zeng H, Ron D. Perk is essential for translational regulation and cell survival during the unfolded protein response. Mol Cell 2000;5:897–904
46. Karaskov E, Scott C, Zhang L, Teodoro T, Ravazzola M, Volchuk A. Chronic palmitate but not oleate exposure induces endoplasmic reticulum stress, which may contribute to Ins-1 pancreatic B-cell apoptosis. Endocrinology 2006;147:3398–3407
47. Jeffrey KD, Alejandro EU, Luciani DS, et al. Carboxypeptidase E mediates palmitate-induced β-cell ER stress and apoptosis. Proc Natl Acad Sci USA 2008;105:8452–8457
48. Luciani DS, Gwiazda KS, Yang TL, et al. Roles of IP3R and RYR Ca2+ channels in endoplasmic reticulum stress and beta-cell death. Diabetes 2009;58:422–432
49. Papa FR. Endoplasmic reticulum stress, pancreatic beta-cell degeneration, and diabetes. Cold Spring Harb Perspect Med 2012;2:a007666
50. Greenwood RH, Mahler RF, Hales CN. Improvement in insulin secretion in diabetes after diazoxide. Lancet 1976;307:444–447
51. Alvarsson M, Sundkvist G, Lager I, et al. Beneficial effects of insulin versus sulphonylurea on insulin secretion and metabolic control in recently diagnosed type 2 diabetic patients. Diabetes Care 2003;26:2231–2237
52. Sargsyan E, Ortsäter H, Thorn K, Bergsten P. Diazoxide-induced β-cell rest reduces endoplasmic reticulum stress in lipotoxic β-cells. J Endocrinol 2008;199:41–50
53. Greenberg ME, Ziff EB. Stimulation of 3T3 cells induces transcription of the c-fos proto-oncogene. Nature 1984;311:433–438
54. Özcan U, Yilmaz E, Özcan L, et al. Chemical chaperones reduce ER stress and restore glucose homeostasis in a mouse model of type 2 diabetes. Science 2006;313:1137–1140

55. McCullough KD, Martindale JL, Klotz L-O, Aw T-Y, Holbrook NJ. Gadd153 sensitizes cells to endoplasmic reticulum stress by down-regulating Bcl2 and perturbing the cellular redox state. Mol Cell Biol 2001;21: 1249–1259
56. Song B, Scheuner D, Ron D, Pennathur S, Kaufman RJ. Chop deletion reduces oxidative stress, improves β cell function, and promotes cell survival in multiple mouse models of diabetes. J Clin Invest 2008;118:3378–3389
57. Shimoda M, Kanda Y, Hamamoto S, et al. The human glucagon-like peptide-1 analogue liraglutide preserves pancreatic beta cells via regulation of cell kinetics and suppression of oxidative and endoplasmic reticulum stress in a mouse model of diabetes. Diabetologia 2011;54:1098–1108
58. Lawrence MC, McGlynn K, Naziruddin B, Levy MF, Cobb MH. Differential regulation of CHOP-10/GADD153 gene expression by MAPK signaling in pancreatic β-cells. Proc Natl Acad Sci USA 2007;104:11518–11525
59. McKimpson WM, Weinberger J, Czerski L, et al. The apoptosis inhibitor ARC alleviates the ER stress response to promote β-cell survival. Diabetes 2013;62:183–193
60. LeRoith D, Taylor SI, Olefsky JM. *Diabetes Mellitus: A Fundamental and Clinical Text*. Philadelphia, Lippincott Williams & Wilkins, 2004